Limited-Fronthaul Cell-Free Massive MIMO with Local MMSE Receiver under Rician Fading and Phase Shifts

Manijeh Bashar*, Pei Xiao*, Rahim Tafazolli*, Kanapathippillai Cumanan†, Alister G. Burr†, and Emil Björnson‡
*University of Surrey, UK, †University of York, UK, ‡Linköping University, Sweden
{m.bashar,p.xiao,r.tafazolli@surrey.ac.uk}@surrey.ac.uk, {kanapathippillai.cumanan,alister.burr}@york.ac.uk, emil.bjornson@liu.se

***Abstract*—A cell-free Massive multiple-input multiple-output (MIMO) system is considered, where the access points (APs) are linked to a central processing unit (CPU) via the limited-capacity fronthaul links. It is assumed that only the quantized version of the weighted signals are available at the CPU. The achievable rate of a limited fronthaul cell-free massive MIMO with local minimum mean square error (MMSE) detection is studied. We study the assumption of uncorrelated quantization distortion, which is commonly used in literature. We show that this assumption will not affect the validity of the insights obtained in our work. To investigate this, we compare the uplink per-user rate with different system parameters for two different scenarios; 1) the exact uplink per-user rate and 2) the uplink per-user rate while ignoring the correlation between the inputs of the quantizers. Finally, we present the conditions which imply that the quantization distortions across APs can be assumed to be uncorrelated.**

I. Introduction

A. Limited-fronthaul Cell-Free Massive MIMO

Cell-free massive multiple-input multiple-output (MIMO) is a promising technique, where large number of distributed access points (APs) serve a much smaller number of users [1]. Similar to the methodology in [2], we model the phase of the line-of-sight (LoS) path as a uniformly distributed random variable, which enables us to take the phase shifts due to mobility and phase noise into account. In [3], the authors investigate the effect of phase shifts in cell-free massive MIMO. An investigation of device-to-device-based cell-free massive MIMO with limited fronthaul links is presented in [4]. The effect of channel aging in cell-free massive MIMO is investigated in [5]. The authors in [6] investigate the performance of perfect-fronthaul cell-free massive MIMO over spatially correlated Rician fading channels. A limited fronthaul cell-free massive MIMO system is investigated, where the access points (APs) send the quantized versions of the received signals and the channel estimates to a central processing unit (CPU) through limited fronthaul links [7]–[11]. The limited capacity links from the APs to the CPU constitute one of the most principal challenges in the cell-free massive MIMO system. The assumption of infinite fronthaul in [1] is not realistic in practice. In the uplink transmission, the fronthaul network will carry quantized signals, which will affect the system performance. This paper therefore provides an approach for the analysis of the effect of fronthaul quantization distortion correlation on the uplink of cell-free massive MIMO.

B. Why Local Minimum Mean Square Error (L-MMSE) Detection?

We study the case when only the quantized version of the weighted signal is available at the CPU which employs local minimum mean square error (L-MMSE) detection. The L-MMSE detection is interesting due to following reasons: **1)** The L-MMSE detector has low complexity and is practically feasible. Note that inversion of the aggregate the channel matrix is required for designing zero forcing (ZF) and MMSE. Hence, due to the large number of users and APs in cell-free massive MIMO, ZF and MMSE detectors impose huge complexity burden on the CPU and they are not suitable for practical implementations. It should be noted that the current hardware cannot perform matrix inversion for a matrix with the dimension larger than 25×25 in practical systems [12], [13]. **2)** The L-MMSE detector provides good performance in cell-free massive MIMO with the use of only the local channel matrix [14]. **3)** The L-MMSE detector can be implemented in a distributed manner, as each AP uses the complex conjugate of the channel estimates in a distributed approach [14]. **4)** The L-MMSE detector can facilitate flexible functional splits in cell-free massive MIMO [15].

This work was supported by the U.K. Engineering and Physical Sciences Research Council under Grant EP/ P03456X/1.

C. Motivation and Contribution

In [16], the authors generalize the Bussgang theorem for MIMO distortions. According to [16], it is common that the quantization distortion correlation is neglected without any justifications and motivations in the literature. In [16], the authors extend the Bussgang results to be applicable hardware impairments [7]. In [16], the authors investigate the cumulative distribution function (CDF) of the absolute value of the correlation coefficient between elements of the MIMO system.

In this paper, we study the performance of a cell-free massive MIMO with the L-MMSE detector. The effect of the quantization distortion correlation on the cell-free massive MIMO system is investigated. In general, the inputs of the quantizers at different APs are correlated, the quantization distortions across APs are therefore correlated. However, according to [9]–[11], the correlation between the inputs of the quantizers at different APs renders, the closed-form achievable rate formulas overly complicated and many optimization problems (i.e., sum-rate maximization, max-min rate, energy efficiency maximization) are intractable. For this reason, in [9]–[11], [17], the quantization distortion correlation is not taken into account and an approximated achievable rate derived by ignoring the quantization distortion correlation is exploited to facilitate the capacity analysis in [9]–[11], [17]. In this paper, we present approximation and exact closed-forms for the capacity of the limited-fronthaul cell-free massive MIMO system to analyze the impact of quantization distortion correlation. However, in this paper, we present the exact definition of the power of the quantization distortion. The analytical and numerical results for typical cases imply that, for cell-free Massive MIMO, under the necessary conditions listed below, the quantization distortions are approximately uncorrelated: **1)** There is a large number of users, or **2)** there are a few antennas at each AP. In this paper, we show that for small number of antennas per AP, the approximation on the achievable rate while ignoring the quantization distortion correlation is very close to the exact achievable rate. However, if there are few active users and each AP is equipped with a large number of antennas, then the correlation between the outputs of the quantizers have a substantial impact on the achievable rate. The approximate rate expression that neglects the correlation should not be used in that case.

II. System Model

We consider uplink transmission in a cell-free massive MIMO system with M APs and K single-antenna users randomly dis-

tributed in a large area. Moreover, we assume each AP has N antennas.

A. Channel Model

The uplink channel between the mth AP and the kth user is presented by $\mathbf{g}_{mk}$ which is modeled as [2]

$$\mathbf{g}_{mk} = \sqrt{\alpha_{mk}} e^{j\phi_{mk}} + \sqrt{\beta_{mk}} \tilde{\mathbf{h}}_{mk}, \tag{1}$$

where $\sqrt{\alpha_{mk}} e^{j\phi_{mk}}$ corresponds to the LoS component and $\sqrt{\beta_{mk}} \tilde{\mathbf{h}}_{mk}$ accounts for the NLoS components. Note that the term $\phi_{mk} \sim [-\pi, \pi)$ is the phase-shift of the LoS component. Moreover, we have $\alpha_{mk} = \frac{\kappa_{mk}}{\kappa_{mk}+1} \zeta_{mk}$ and $\beta_{mk} = \frac{1}{\kappa_{mk}+1} \zeta_{mk}$, where ζ_{mk} denotes the large-scale fading coefficient. In addition, the term κ_{mk} is modelled as [2]

$$\kappa_{mk} = \frac{P_{\text{LoS}}(d_{mk})}{1 + P_{\text{LoS}}(d_{mk})}, \tag{2}$$

where d_{mk} is the distance between the mth AP and the kth user, $P_{\text{LoS}}(d_{mk})$ is the LoS probability depending on the distance d_{mk}, where the LoS probability is defined in Section III.

B. Channel Estimation at the APs

All pilot sequences transmitted by the K users in the channel estimation phase are collected in a matrix $\mathbf{\Phi} \in \mathbb{C}^{\tau_p \times K}$, where τ_p is the length of the pilot sequence for each user and the kth column, $\boldsymbol{\phi}_k$, represents the pilot sequence used by the kth user, where $\|\boldsymbol{\phi}_k\|^2 = 1$. Let $\sqrt{\tau}\boldsymbol{\phi}_k \in \mathbb{C}^{\tau \times 1}$ be the pilot sequence assigned to the kth user. We assume the case where channel statistics are available at the APs, however, the phase shifts are completely unknown. Then, we can use the non-aware linear MMSE (LMMSE) estimator. Based on the analysis in [2, Section III-B], the LMMSE estimate of the channel $\mathbf{g}_{mk}$ is given by

$$\hat{\mathbf{g}}_{mk} = c_{mk} \Big(\sqrt{\tau_p p_p} \mathbf{g}_{mk} + \sqrt{\tau_p p_p} \sum_{k' \neq k}^{K} \mathbf{g}_{mk'} \boldsymbol{\phi}_{k'}^H \boldsymbol{\phi}_k \mathbf{\Omega}_{p,m} \boldsymbol{\phi}_k \Big), \tag{3}$$

where $\mathbf{\Omega}_{p,m}$ denotes the noise vector at the mth AP whose elements are independent and identically distributed (i.i.d.) $\mathcal{CN}(0,1)$, p_p represents the normalized signal-to-noise ratio (SNR) of each pilot symbol. The $\bar{p}_p$ denotes the power of pilot sequence where $p_p = \frac{\bar{p}_p}{p_n}$ and p_n is the noise power [18]. Moreover, we have $c_{mk} = \frac{\sqrt{\tau_p p_p}(\beta_{mk} + \alpha_{mk})}{\tau_p p_p \sum_{k'=1}^{K} (\beta_{mk'} + \alpha_{mk'}) |\boldsymbol{\phi}_{k'}^H \boldsymbol{\phi}_k|^2 + 1}$ and $\gamma_{mk} = \sqrt{\tau_p p_p} c_{mk} (\beta_{mk} + \alpha_{mk})$.

C. Data Detection

The transmitted signal from the kth user is denoted by $x_k = \sqrt{\rho\ q_k} s_k$, where s_k with $\mathcal{CN}(0,1)$ and q_k denotes the transmitted symbol and the transmit power, respectively. Moreover, ρ refers to the normalized uplink SNR. The $N \times 1$ received signal at the mth AP is given by

$$\mathbf{y}_m = \sqrt{\rho} \sum_{k=1}^{K} \mathbf{g}_{mk} \sqrt{q_k} s_k + \mathbf{n}_m, \tag{4}$$

where $\mathbf{n}_m \sim \mathcal{CN}(\mathbf{0}, \mathbf{I}_N)$ is the noise vector at the mth AP. We consider the case when each AP multiplies the received signal by the L-MMSE receiver, and sends back a quantized version of this weighted signal to the CPU. Let $\mathbf{v}_{mk} \mathbb{C}^N$ be the L-MMSE vector that the mth AP design for the kth user. Then the local estimate of the transmitted signal s_k, i.e., $\hat{s}_{mk}$, is given by

$$z_{mk} \triangleq \hat{s}_{mk} = \mathbf{v}_{mk}^H \mathbf{y}_m, \tag{5}$$

where

$$\mathbf{v}_{mk} = \left(\tilde{a}^2 \rho \sum_{k'=1}^{K} q_{k'} \hat{\mathbf{g}}_{mk'} \hat{\mathbf{g}}_{mk'}^H + \mathbf{R}_{mk} \right)^{-1} \hat{\mathbf{g}}_{mk}, \tag{6}$$

where $\mathbf{R}_{mk} = \rho \sum_{k'=1}^{K} q_{k'} \mathbf{W}_{mk'} + \mathbf{I}_N + \mathbf{F}_m$ and

$$\mathbf{W}_{mk'} = \mathbf{S}_{mk'} - \mathbf{T}_{mk'}, \tag{7a}$$

$$\mathbf{S}_{mk'} = \left(\frac{\sigma_{\tilde{e},\text{B}}^2}{\tilde{a}^2} + 1 \right) \text{diag}\left[\text{rep}\left(\beta_{mk'} + \alpha_{mk'}, N \right) \right], \tag{7b}$$

$$\mathbf{T}_{mk'} = \left(1 - \sigma_{\tilde{e},\text{B}}^2 \right) \text{diag}\left[\text{rep}\left(\gamma_{mk'}, N \right) \right], \mathbf{F}_m = \frac{\sigma_{\tilde{e},\text{B}}^2}{\tilde{a}^2} \mathbf{I}_N, \tag{7c}$$

where $\tilde{a}$ and $\sigma_{\tilde{e},\text{B}}^2$ are the constant term in the Bussgang decomposition and the quantization distortion power, respectively, which are defined in [9, Table 1]. The mth AP quantizes the terms $z_{mk} = \mathbf{v}_{mk}^H \mathbf{y}_m, \forall k$, and forwards the quantized signals in each symbol duration to the CPU, where $\mathbf{v}_{mk}$ is the L-MMSE receiver. Hence z_{mk} is the input of the quantizer at the mth AP. Using the Bussgang decomposition, the estimate of the signal s_k at the CPU can be written as

$$\begin{aligned} \hat{s}_k &= \sum_{m=1}^{M} \mathcal{Q}\left(z_{mk} \right) = \sum_{m=1}^{M} \mathcal{Q}\left(\mathbf{v}_{mk}^H \mathbf{y}_m \right) \\ &= \sum_{m=1}^{M} \tilde{a} \mathbf{v}_{mk}^H \mathbf{y}_m + \underbrace{\sum_{m=1}^{M} d_{mk}^z}_{\text{TQD}_k}, \end{aligned} \tag{8}$$

where TQD_k refers to the total quantization distortion (TQD) at the kth user. Since the input to the quantizer is the sum of many random variables, from the central limit theorem, it has a nearly Gaussian distribution [10]. Moreover, using Bussgang decomposition the elements of the quantization distortion are uncorrelated with the input of the quantizer [19], i.e.,

$$\mathbb{E}\left\{ \left(\mathbf{v}_{mk}^H \mathbf{y}_m \right)^H d_{mk}^z \right\} = 0. \tag{9}$$

The achievable rate of the kth user is given by $R_k = \log_2(1 + \text{SINR}_k)$, where the SINR_k is the achievable signal-to-interference-plus-noise ratio (SINR) of the kth user and is given by

$$\text{SINR}_k = \frac{q_k \underline{\mathbf{1}}^T \bar{\mathbf{f}}_{kk} \bar{\mathbf{f}}_{kk}^H \underline{\mathbf{1}}}{\sum_{k'=1}^{K} q_{k'} \mathbb{E}\{ \underline{\mathbf{1}}^T \bar{\mathbf{f}}_{kk'} \bar{\mathbf{f}}_{kk'}^H \underline{\mathbf{1}}^T \} - q_k \underline{\mathbf{1}}^T \bar{\mathbf{f}}_{kk} \bar{\mathbf{f}}_{kk}^H \underline{\mathbf{1}} + \frac{1}{\rho} \sum_{m=1}^{M} \underline{\mathbf{1}}^T \mathbf{D}_k \underline{\mathbf{1}} + \frac{1}{\rho} \mathbb{E}\left\{ |\text{TQD}_k|^2 \right\}}, \tag{10}$$

where $\bar{\mathbf{f}}_{kk'} = \left[\mathbb{E}\{\mathbf{v}_{1k}^H \hat{\mathbf{g}}_{1k'}\} \cdots \mathbb{E}\{\mathbf{v}_{Mk}^H \hat{\mathbf{g}}_{Mk'}\} \right]^T$, $\mathbf{D}_k = \text{diag}\left[\mathbb{E}\left\{ ||\mathbf{v}_{1k}||^2 \right\} \cdots \mathbb{E}\left\{ ||\mathbf{v}_{Mk}||^2 \right\} \right]^T$ where $\underline{\mathbf{1}} = [1, \cdots, 1]^T \in \mathbb{C}^N$. The power of the quantization distortion for user k is given by

$$\begin{aligned} \mathbb{E}\left\{ |\text{TQD}_k|^2 \right\} &= \mathbb{E}\left\{ \left| \sum_{m=1}^{M} d_{mk}^z \right|^2 \right\} \\ &= \mathbb{E}\left\{ \left(\sum_{m=1}^{M} d_{mk}^z \right) \left(\sum_{m=1}^{M} d_{mk}^z \right)^* \right\} \\ &= \sum_{m=1}^{M} \mathbb{E}\left\{ |d_{mk}^z|^2 \right\} + \sum_{m=1}^{M} \sum_{n \neq m}^{M} \mathbb{E}\left\{ d_{mk}^z \left(d_{nk}^z \right)^* \right\} \\ &= \sum_{m=1}^{M} \left[\mathbf{C}_{\mathbf{d}_k^z \mathbf{d}_k^z} \right]_{mm} + \sum_{m=1}^{M} \sum_{n \neq m}^{M} \left[\mathbf{C}_{\mathbf{d}_k^z \mathbf{d}_k^z} \right]_{nm}, \end{aligned} \tag{11}$$

where $\mathbf{C}_{\mathbf{d}_k^z \mathbf{d}_k^z} = \mathbb{E}\left\{ \mathbf{d}_k^z \left(\mathbf{d}_k^z \right)^H \right\}$ is the covariance matrix of the quantization distortion and $\mathbf{d}_k^z = [d_{1k}^z \cdots d_{Mk}^z]^T$ is the quantization distortion vector. Note that $\left[\mathbf{C}_{\mathbf{d}_k^z \mathbf{d}_k^z} \right]_{mn}$ is the mnth element of $\mathbf{C}_{\mathbf{d}_k^z \mathbf{d}_k^z}$. To calculate $\mathbf{C}_{\mathbf{d}_k^z \mathbf{d}_k^z}$, we first re-write the aggregate received signal at the CPU as follows:

$$\mathbf{r}_k = Q(\mathbf{z}_k) = \mathbf{A} \mathbf{z}_k + \mathbf{d}_k^z, \tag{12}$$

where $\mathbf{r}_k = [r_{1k} \cdots r_{Mk}]^T$ and $\mathbf{z}_k = [z_{1k} \cdots z_{Mk}]^T$. Moreover, based on the analysis in [20], it can be shown that the matrix $\mathbf{A}$ is

diagonal. The matrix $\mathbf{A}$ is determined by the LMMSE estimation of $\mathbf{r}_k$ from $\mathbf{z}_k$ as follows [20]:

$$\mathbf{A} = \mathbb{E}\left\{\mathbf{r}_k \mathbf{z}_k^H\right\} \mathbb{E}\left\{\mathbf{z}_k \mathbf{z}_k^H\right\}^{-1} = \mathbf{C}_{\mathbf{r}_k \mathbf{z}_k} \mathbf{C}^{-1}_{\mathbf{d}_k^z \mathbf{d}_k^z}, \tag{13}$$

and the error has the following covariance matrix [20]

$$\begin{aligned}\mathbf{C}_{\mathbf{d}_k^z \mathbf{d}_k^z} &= \mathbb{E}\left\{\left(\mathbf{r}_k - \mathbf{A}\mathbf{z}_k\right)\left(\mathbf{r}_k - \mathbf{A}\mathbf{z}_k\right)^H\right\} \mathbb{E}\left\{\mathbf{z}_k \mathbf{z}_k^H\right\}^{-1} \\ &= \mathbf{C}_{\mathbf{r}_k \mathbf{r}_k} - \mathbf{C}_{\mathbf{r}_k \mathbf{z}_k} \mathbf{A}^H - \mathbf{A}\mathbf{C}_{\mathbf{z}_k \mathbf{r}_k} + \mathbf{A}\mathbf{C}_{\mathbf{z}_k \mathbf{z}_k} \mathbf{A}^H \\ &= \mathbf{C}_{\mathbf{r}_k \mathbf{r}_k} - \mathbf{C}_{\mathbf{r}_k \mathbf{z}_k} \mathbf{C}^{-1}_{\mathbf{z}_k \mathbf{z}_k} \mathbf{C}_{\mathbf{z}_k \mathbf{r}_k}. \end{aligned} \tag{14}$$

Proposition 1. *The covariance matrices $\mathbf{C}_{\mathbf{r}_k \mathbf{r}_k}$, $\mathbf{C}_{\mathbf{r}_k \mathbf{z}_k}$, and $\mathbf{C}_{\mathbf{z}_k \mathbf{r}_k}$ are obtained using the Price Theorem.*

Proof: To characterize the cross-correlation and auto-correlation properties of Gaussian input signals, we exploit *the Price Theorem* [21]. Based on the Price theorem, the correlation coefficient at the output of nonlinear functions $f_1(x_1)$ and $f_2(x_2)$ with correlated inputs x_1 and x_2 having zero-mean and the variances σ_1 and σ_2, respectively, and the correlation coefficient $\rho_{x_1 x_2} = \frac{\mathbb{E}\{x_1 x_2^*\}}{\sigma_{x_1} \sigma_{x_2}}$, has the following derivatives [21]

$$\frac{\partial^k \mathbb{E}\left\{f_1(x_1) f_2(x_2)\right\}}{\partial \rho_{x_1 x_2}^k} = \sigma_1^k \sigma_2^k \int_{-\infty}^{\infty}\int_{-\infty}^{\infty} \frac{f_1^{(k)}(x_1) f_2^{(k)}(x_2)}{2\pi\sigma_1\sigma_2\sqrt{1-\rho_{x_1 x_2}^2}}$$
$$\exp\left(-\frac{1}{2\left(1-\rho_{x_1 x_2}^2\right)}\left[\frac{x_1^2}{\sigma_1^2} + \frac{x_2^2}{\sigma_2^2} - \frac{2\rho_{x_1 x_2} x_1 x_2}{\sigma_1\sigma_2}\right]\right) dx_1 dx_2. \tag{15}$$

Next, for the special case $f_1(x_1) = x_1$, then we have [20]

$$\frac{\partial \mathbb{E}\left\{x_1 f_2(x_2)\right\}}{\partial \rho_{x_1 x_2}} = \sigma_1\sigma_2 \int_{-\infty}^{\infty} \frac{1}{\sigma_2\sqrt{2\pi}} f_2'(x_2) \exp\left(\frac{x_2^2}{\sigma_2^2}\right) dx_2, \tag{16}$$

resulting in

$$\mathbb{E}\left\{x_1 f_2(x_2)\right\} = \sigma_1\sigma_2\rho_{x_1 x_2} \int_{-\infty}^{\infty} \frac{1}{\sigma_2\sqrt{2\pi}} f_2'(x_2) \exp\left(\frac{x_2^2}{\sigma_2^2}\right) dx_2. \tag{17}$$

Next, we use the uniform quantizer as follows [20, Chapter 2]

$$\begin{aligned} f_2(x) = Q(x) &= \sum_{i=1}^{2^\alpha} l^i \left(u\left(x - l^{\text{lo},i}\right) - u\left(x - l^{\text{up},i}\right)\right) \\ &= l^1 + \sum_{i=2}^{2^\alpha} \left(l^i - l^{i-1}\right) u\left(x - l^{\text{lo},i}\right). \end{aligned} \tag{18}$$

Using the $l^{\text{up},i} = l^{\text{lo},i+1}$, we have

$$\frac{\partial Q(x)}{\partial x} = l^1 + \sum_{i=2}^{2^\alpha} \left(l^i - l^{i-1}\right) \delta\left(x - l^{\text{lo},i}\right), \tag{19}$$

where δ is the Dirac Delta function. Therefore

$$\mathbb{E}\left\{x_1 Q(x_2)\right\} = \sigma_1\rho_{x_1 x_2} \sum_{i=1}^{2^\alpha} \frac{l^i \left(\exp\left(-\frac{\left(l^{\text{lo},i}\right)^2}{2\sigma_2^2}\right) - \exp\left(-\frac{\left(l^{\text{up},i}\right)^2}{2\sigma_2^2}\right)\right)}{\sqrt{2\pi}}. \tag{20}$$

Next, we find the covariance at the output of the quantizer as follows

$$\mathbb{E}\left\{Q(x_1)Q(x_2)\right\} = \sum_{i=2}^{K}\sum_{k=2}^{K} \Delta^2 \int_0^{\rho_{x_1 x_2}} \frac{\exp\left(-\frac{1}{2(1-\rho'^2)}\left[\frac{\left(l^{\text{lo},i}\right)^2}{\sigma_1^2} + \frac{\left(l^{\text{lo},k}\right)^2}{\sigma_2^2} - \frac{2\rho' l^{\text{lo},i} l^{\text{lo},k}}{\sigma_1\sigma_2}\right]\right)}{2\pi\sqrt{1-\rho'^2}} d\rho'. \tag{21}$$

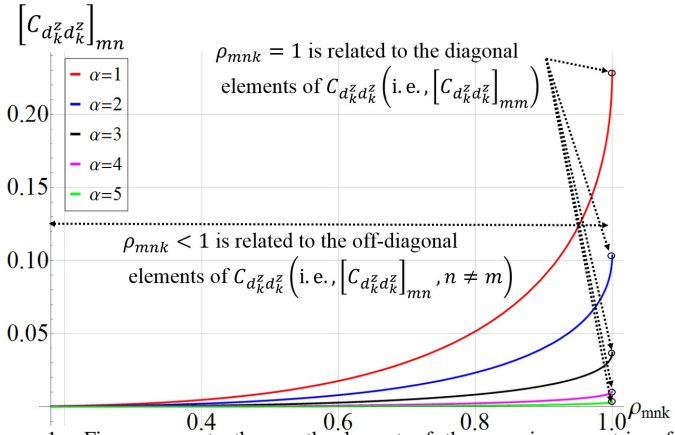

Figure 1. Figure presents the mnth element of the covariance matrix of the quantization distortion (i.e., $\left[\mathbf{C}_{\mathbf{d}_k^z \mathbf{d}_k^z}\right]_{mn}$ in (11)) versus ρ_{mnk} for different number of quantization bits for a given user k.

Note that in cell-free Massive MIMO, we have $\rho_{x_1 x_2} = \rho_{mnk}$, where ρ_{mnk} is defined in (24). Finally, $\mathbf{C}_{\mathbf{r}_k \mathbf{r}_k}$, $\mathbf{C}_{\mathbf{r}_k \mathbf{z}_k}$ and $\mathbf{C}_{\mathbf{z}_k \mathbf{r}_k}$ are determined using (20) and (21) and the following equalities:

$$\mathbf{C}_{\mathbf{r}_k \mathbf{r}_k} = \mathbb{E}\left\{\mathbf{r}_k \mathbf{r}_k\right\} = \mathbb{E}\left\{Q(\mathbf{z}_k) Q(\mathbf{z}_k)\right\}, \tag{22a}$$

$$\mathbf{C}_{\mathbf{z}_k \mathbf{r}_k} = \mathbb{E}\left\{\mathbf{z}_k \mathbf{r}_k\right\} = \mathbb{E}\left\{\mathbf{z}_k Q(\mathbf{z}_k)\right\}, \tag{22b}$$

$$\mathbf{C}_{\mathbf{r}_k \mathbf{z}_k} = \mathbb{E}\left\{\mathbf{r}_k \mathbf{z}_k\right\} = \mathbb{E}\left\{Q(\mathbf{z}_k) \mathbf{z}_k\right\}, \tag{22c}$$

which completes the proof. ■

Based on the above derivations, $\left[\mathbf{C}_{\mathbf{d}_k^z \mathbf{d}_k^z}\right]_{mn}$ is a function of the number of quantization bits α, the step-size of the quantizer Δ, and the correlation coefficient between the inputs of the quantizer at the mth and nth APs, i.e., ρ_{mnk}, which is obtained numerically.

III. Numerical Results and Discussion

A cell-free Massive MIMO system with M APs and K single-antenna users is considered in a $D \times D$ numerical area, where both APs and users are uniformly distributed at random points. The path loss and noise power are the same as [1]. For the LoS probability, we use the following model from the 3GPP-UMa [2]

$$P_{\text{LoS}}(d_{mk}) = \min\left(\frac{18}{d_{mk}}, 1\right)\left(1 - e^{-\frac{d_{mk}}{63}}\right) + e^{-\frac{d_{mk}}{63}}, \tag{23}$$

where d_{mk} is in meters. In cell-free massive MIMO, the inputs of quantizer at the mth and nth APs are $z_{mk} = \mathbf{v}_{mk}^H \mathbf{y}_m$ and $z_{nk} = \mathbf{v}_{nk}^H \mathbf{y}_n$, respectively. We aim to calculate the correlation coefficient between the mth and nth APs, which is given by

$$\rho_{mnk} = \frac{\left|\mathbb{E}\left\{z_{mk} z_{nk}^*\right\}\right|}{\sigma_{z_{mk}} \sigma_{z_{nk}}}, \tag{24}$$

where we have $\sigma_{z_{mk}}^2 = \mathbb{E}\left\{\left|z_{mk}\right|^2\right\}$, and the expectation is taken over the small-scale fading coefficients.

1) The Actual Value of Correlation Between the Quantization Distortions Versus the Correlation Between the Inputs of the Quantizers: Fig. 1 plots $\left[\mathbf{C}_{\mathbf{d}_k^z \mathbf{d}_k^z}\right]_{mn}$ versus ρ_{mnk} for different numbers of quantization bits α, where the diagonal elements of the covariance matrix are obtained by setting $\rho_{mnk} = 1$. Fig. 1 plots $\left[\mathbf{C}_{\mathbf{d}_k^z \mathbf{d}_k^z}\right]_{mn}$ versus ρ_{mnk} for different numbers of quantization bits α, where the diagonal elements of the covariance matrix are obtained by setting $\rho_{mnk} = 1$. From Fig. 1, it can be observed that $\rho_{mnk} \leq 0.4$ is small enough so that the off-diagonal elements of the correlation matrix can be safely ignored. Note that the performance gap between the exact uplink per-user rate and the uplink per-user rate while ignoring the correlation between the inputs of quantizers depend on total

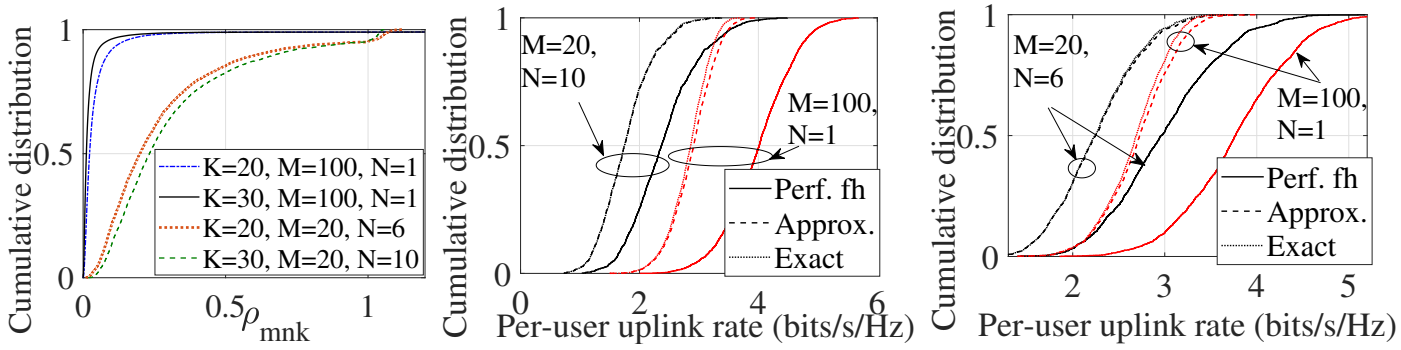

(a) CDF of ρ_{mnk}, given in (24). (b) $K = 20$. (c) $K = 30$.

Figure 2. The term "Perf. fh" refers to the perfect fronthaul link. The term "Exact" is the case where we include the correlation between the quantization distortions at different APs whereas the term "Approx." refers to the case when we ignore the correlations between the error at different APs.

number of users in the area K and the number of antennas per-AP N. Hence, in the next section, we investigate the effect of K and N on the correlation coefficients ρ_{mnk} and the achievable rate. Next, we provide numerical results and discussion to address the effect of correlation between the inputs of the quantizers at different APs.

2) How Large is the Correlation Between the Input of the Quantizers at Different APs in Cell-Free Massive MIMO?: The CDF of ρ_{mnk} in cell-free Massive MIMO for the cases of $K = 20$ and $K = 30$ users is plotted in Fig. 2a. The figure shows that in the case of a few antennas per AP and large number of users in the area, the correlation between the inputs of the quantizer at different APs is small. The correlation coefficient ρ_{mnk} enables us to investigate the performance gap between the exact rate and the approximated rate obtained by omitting the correlation ρ_{mnk}. Note that by increasing the number of APs, the correlation ρ_{mnk} decreases, resulting in a smaller gap between the approximated rate and the exact rate. This will be investigated in the next subsection.

3) The Performance Gap Between the Exact Uplink Per-User Rate and the Uplink Per-User Rate While Ignoring the Correlation Between the Inputs of the Quantizers: In this section, we present the uplink per-user rate with different system parameters for two different scenarios. To remind, the correlation between the quantization distortions at different APs is given by

$$\mathbb{E}\left\{|\mathrm{TQD}_k|^2\right\} = \sum_{m=1}^{M}\left[\mathbf{C}_{\mathbf{d}_k^z\mathbf{d}_k^z}\right]_{mm} + \sum_{m=1}^{M}\sum_{n\neq m}^{M}\left[\mathbf{C}_{\mathbf{d}_k^z\mathbf{d}_k^z}\right]_{nm}. \tag{25}$$

The rate obtained by the exact value of $\mathbb{E}\left\{|\mathrm{TQD}_k|^2\right\}$ in (26) is referred to as "Exact" in Figs. 2b-2c. Next, we exploit the results in Figs. 2b-2c, the covariance matrix of the quantization distortion is approximated with a diagonal matrix as follows:

$$\mathbb{E}\left\{|\mathrm{TQD}_k|^2\right\} = \underbrace{\sum_{m=1}^{M}\left[\mathbf{C}_{\mathbf{d}_k^z\mathbf{d}_k^z}\right]_{mm}}_{\text{sum of diagonal elements of } \mathbf{C}_{\mathbf{d}_k^z\mathbf{d}_k^z}} + \underbrace{\sum_{m=1}^{M}\sum_{n\neq m}^{M}\left[\mathbf{C}_{\mathbf{d}_k^z\mathbf{d}_k^z}\right]_{nm}}_{\text{sum of off-diagonal elements of } \mathbf{C}_{\mathbf{d}_k^z\mathbf{d}_k^z}} \approx \sum_{m=1}^{M}\left[\mathbf{C}_{\mathbf{d}_k^z\mathbf{d}_k^z}\right]_{mm}. \tag{26}$$

This scenario is given as "Approximation" in Figs. 2b-2c. As Figs. 2b-2c show, there is a negligible performance gap between the exact rate and the approximate rate obtained by ignoring the quantization distortion correlation. Here we consider the uncorrelated quantization distortions at different APs, and the total quantization distortion is obtained as follows:

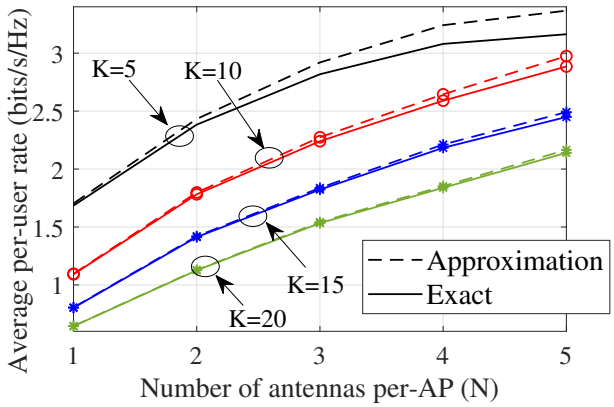

Figure 3. This figure presents the average uplink per-user rate versus number of antennas per AP with $M = 15$ and $\alpha = 1$. Here the term "Exact" refers to the exact uplink rate whereas the term "Approximation" presents the uplink per-user rate while ignoring the quantization correlation.

$$\mathbb{E}\left\{|\mathrm{TQD}_k|^2\right\} = \mathbb{E}\left\{\left|\sum_{m=1}^{M} d_{mk}^z\right|^2\right\} \tag{27}$$

$$\approx \sum_{m=1}^{M}\mathbb{E}\left\{|d_{mk}^z|^2\right\} = \left(\tilde{b}-\tilde{a}^2\right) \sum_{m=1}^{M}\left[N^2\sum_{k'=1}^{K}\gamma_{mk'}^2\left|\boldsymbol{\phi}_{k'}^H\boldsymbol{\phi}_k\right|^2\rho q_{k'} + N\gamma_{mk}\sum_{k'=1}^{K}\beta_{mk'}\rho q_{k'} + N\gamma_{mk}\right].$$

Next, we investigate the ratio between "the sum of off-diagonal elements of the distortion covariance matrix" and "the sum of all elements of the distortion covariance matrix" in (26). We define the following ratio:

$$\mathrm{ratio}_C = \frac{\sum_{m=1}^{M}\sum_{n\neq m}^{M}\left[\mathbf{C}_{\mathbf{d}_k^z\mathbf{d}_k^z}\right]_{nm}}{\sum_{m=1}^{M}\left[\mathbf{C}_{\mathbf{d}_k^z\mathbf{d}_k^z}\right]_{mm} + \sum_{m=1}^{M}\sum_{n\neq m}^{M}\left[\mathbf{C}_{\mathbf{d}_k^z\mathbf{d}_k^z}\right]_{nm}}. \tag{28}$$

Fig. 4 demonstrates the cumulative distribution of ratio_C with the same parameters as in Fig. 3. Moreover, Fig. 4 shows that the power of the off-diagonal elements of the quantization distortion matrix is very small relative to the power of all elements of the quantization distortion matrix, except for smaller K and larger N. This explains the performance gap between the systems using "Approximation" (obtained by ignoring off-diagonal elements of the distortion covariance matrix) and "Exact" in Fig. 3.

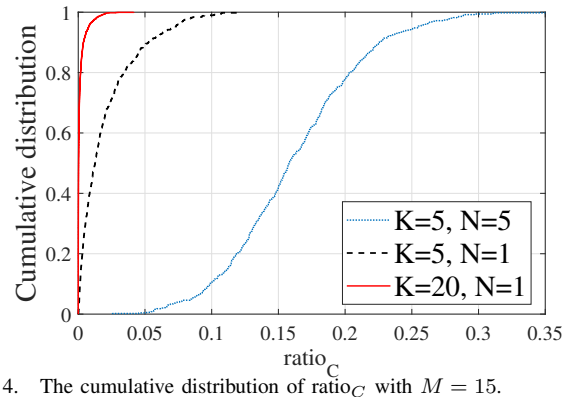

Figure 4. The cumulative distribution of ratio$_C$ with $M = 15$.

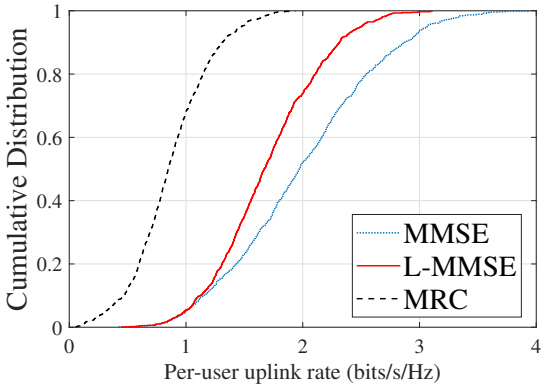

Figure 5. The average uplink per-user rate with three different detectors with $M = 60$, $N = 1$, and $K = 20$.

4) The effects of number of users and number of antennas per AP: Finally, we investigate the effect of the total number of users and number of antennas per AP on the system performance. In Fig. 3, the average per-user uplink rate is presented versus the number of antennas per AP (N) for different cases of total number of users in the system (namely $K = \{5, 10, 15, 20\}$). As the figure shows for the case of single antenna APs, the average uplink per-user rate while omitting the quantization correlation is very close to the exact uplink per-user rate. Moreover, as the figure demonstrates, if there are $K \leq 10$ active users in the area, the average uplink per-user rate while omitting the quantization correlation (shown as Approximation in the figure) is very close to the exact rate. As a results, if there are $K < 10$ active users and the AP are equipped with $N > 2$ antennas, the correlation between the inputs of the quantizers should not be ignored.

5) The effect of different linear detectors: This section investigates the average uplink per-user rate of cell-free massive MIMO with three different receivers, namely the MMSE, L-MMSE and MRC receivers. In Fig. 5, we assume that $M = 40$ APs each with $N = 2$ antennas are uniformly distributed in the area. Moreover, we consider $K = 20$ users and $\tau_p = 20$ as the length of pilot sequences. As the figure shows the MMSE receiver provides the greatest median uplink rate. Note that in the case of MRC and L-MMSE, the CPU does not have access to the quantized channel estimates and exploits only the statistics of the channel to decode the data whereas to design the MMSE receiver the CPU needs to have the quantized version of channel to design the receiver.

IV. Conclusions

We have considered cell-free massive MIMO with L-MMSE detector, when the quantized version of the weighted signals are available at the CPU. Bussgang decomposition has been used to model the quantization effects. We have investigated the assumption of uncorrelated quantization distortion and showed that this assumption will not affect the insights obtained in our works. We presented a comparison between the exact uplink per-user rate and the uplink per-user rate while ignoring the correlation between the inputs of the quantizers. Finally, we have presented the conditions which imply that the quantization distortions across APs can be considered as uncorrelated signals.

References

[1] H. Q. Ngo, A. Ashikhmin, H. Yang, E. G. Larsson, and T. L. Marzetta, "Cell-free massive MIMO versus small cells," *IEEE Trans. Wireless Commun.*, vol. 16, no. 3, pp. 1834–1850, Mar. 2017.

[2] Özdogan, E. Björnson, and J. Zhang, "Performance of cell-free massive MIMO with rician fading and phase shifts," *IEEE Trans. Wireless Commun.*, vol. 18, no. 11, pp. 5299–5315, Nov. 2019.

[3] O. T. Demir and E. Björnson, "Large-scale fading precoding for spatially correlated rician fading with phase shifts," in *Proc. IEEE ICASSP*, May 2020, pp. 5150–5154.

[4] H. Masoumi, M. J. Emadi, and S. Buzzi, "Cell-free massive MIMO with underlaid D2D communications and low resolution ADCs," *Available: https://arxiv.org/pdf/2005.10068.pdf*.

[5] J. Zheng, J. Zhang, E. Björnson, and B. Ai, "Cell-free massive MIMO with channel aging and pilot contamination," in *Proc. IEEE Globecom*, Dec. 2020, pp. 1–6.

[6] Z. Wang, J. Zhang, E. Björnson, and B. Ai, "Uplink performance of cell-free massive MIMO over spatially correlated rician fading channels," *IEEE Wireless Commun. Lett.*, pp. 1–5, To appear.

[7] H. Masoumi and M. J. Emadi, "Performance analysis of cell-free massive MIMO system with limited fronthaul capacity and hardware impairments," *IEEE Trans. Wireless Commun.*, vol. 19, no. 2, pp. 1038–1053, Feb. 2020.

[8] M. Guenach, A. A. Gorji, and A. Bourdoux, "Joint power control and access point scheduling in fronthaul-constrained uplink cell-free massive MIMO systems," *IEEE Trans. Commun.*, vol. 69, no. 4, pp. 2709–2722, Apr. 2021.

[9] M. Bashar, K. Cumanan, A. G. Burr, H. Q. Ngo, and M. Debbah, "Max-min SINR of cell-free massive MIMO uplink with optimal uniform quantization," *IEEE Trans. Commun.*, vol. 67, no. 10, pp. 6796–6815, Oct. 2019.

[10] M. Bashar, K. Cumanan, A. G. Burr, H. Q. Ngo, E. G. Larsson, and P. Xiao, "Energy efficiency of the cell-free massive MIMO uplink with optimal uniform quantization," *IEEE Trans. Green Commun. and Net.*, pp. 1–18, Sep. 2019.

[11] M. Bashar, K. Cumanan, A. G. Burr, H. Q. Ngo, and M. Debbah, "Cell-free massive MIMO with limited backhaul," in *Proc. IEEE ICC*, May 2018, pp. 1–7.

[12] H. Prabhu, O. Edfors, J. Rodrigues, L. Liu, and F. Rusek, "Hardware efficient approximative matrix inversion for linear pre-coding in massive MIMO," in *Proc. IEEE ISCAS*, Jun. 2014, pp. 1700–1703.

[13] S. Chetan, J. Manikandan, V. Lekshmi, and S. Sudhakar, "Hardware implementation of floating point matrix inversion modules on FPGAs," in *Proc. IEEE ICM*, Dec. 2020, pp. 1–4.

[14] E. Björnson and L. Sanguinetti, "Joint power allocation and load balancing optimization for energy-efficient cell-free massive MIMO networks," *IEEE Trans. Wireless Commun.*, vol. 19, no. 10, pp. 77–90, Oct. 2020.

[15] M. Bashar, H. Q. Ngo, K. Cumanan, A. G. Burr, P. Xiao, E. Björnson, and E. G. Larsson, "Uplink spectral and energy efficiency of cell-free massive MIMO with optimal uniform quantization," *IEEE Trans. Commun.*, pp. 1–21, Oct. 2020.

[16] O. T. Demir and E. Björnson, "The Bussgang decomposition of non-linear systems: Basic theory and MIMO extensions," *To appear in Signal Processing Magazine*.

[17] M. Bashar, A. Akbari, K. Cumanan, H. Q. Ngo, A. G. Burr, P. Xiao, M. Debbah, and J. Kittler, "Exploiting deep learning in limited-fronthaul cell-free massive MIMO uplink," *IEEE J. Sel. Areas Commun.*, vol. 38, no. 8, pp. 1678–1697, Jun. 2020.

[18] H. Q. Ngo, L. Tran, T. Q. Duong, M. Matthaiou, and E. G. Larsson, "On the total energy efficiency of cell-free massive MIMO," *IEEE Trans. Green Commun. and Net.*, vol. 2, no. 1, pp. 25–39, Mar. 2017.

[19] P. Zillmann, "Relationship between two distortion measures for memoryless nonlinear systems," *IEEE Signal Process. Lett.*, vol. 17, no. 11, pp. 917–920, Feb. 2010.

[20] A. Mezghani, *Information theoretic Analysis and Signal Processing Techniques for Quantized MIMO Communications*. Ph.D. dissertation, Technical University of Munich, Germany, 2015.

[21] R. Price, "A useful theorem for nonlinear devices having gaussian inputs," *IEEE Trans. Inf. Theory*, vol. 4, no. 2, pp. 69–72, Jun. 1958.